JACS
JOURNAL OF THE AMERICAN CHEMICAL SOCIETY
Article
pubs.acs.org/JACS

A Stepwise Solvent-Promoted S_Ni Reaction of α-D-Glucopyranosyl Fluoride: Mechanistic Implications for Retaining Glycosyltransferases

Jefferson Chan, Ariel Tang, and Andrew J. Bennet*

Department of Chemistry, Simon Fraser University, 8888 University Drive, Burnaby, BC V5A 1S6, Canada

Supporting Information

ABSTRACT: The solvolysis of α-D-glucopyranosyl fluoride in hexafluoro-2-propanol gives two products, 1,1,1,3,3,3-hexafluoropropan-2-yl α-D-glucopyranoside and 1,6-anhydro-β-D-glucopyranose. The ratio of these two products is essentially unchanged for reactions that are performed between 56 and 100 °C. The activation parameters for the solvolysis reaction are as follows: $\Delta H^{\ddagger} = 81.4 \pm 1.7$ kJ mol^{-1}, and $\Delta S^{\ddagger} = -90.3 \pm 4.6$ J mol^{-1} K^{-1}. To characterize, by use of multiple kinetic isotope effect (KIE) measurements, the TS for the solvolysis reaction in hexafluoro-2-propanol, we synthesized a series of isotopically labeled α-D-glucopyranosyl fluorides. The measured KIEs for the C1 deuterium, C2 deuterium, C5 deuterium, anomeric carbon, ring oxygen, O6, and solvent deuterium are 1.185 ± 0.006, 1.080 ± 0.010, 0.987 ± 0.007, 1.008 ± 0.007, 0.997 ± 0.006, 1.003 ± 0.007, and 1.68 ± 0.07, respectively. The transition state for the solvolysis reaction was modeled computationally using the experimental KIE values as constraints. Taken together, the reported data are consistent with the retained solvolysis product being formed in an S_Ni ($D_N^{\ddagger}$*A_{Nss}) reaction with a late transition state in which cleavage of the glycosidic bond is coupled to the transfer of a proton from a solvating hexafluoro-2-propanol molecule. In comparison, the inverted product, 1,6-anhydro-β-D-glucopyranose, is formed by intramolecular capture of a solvent-equilibrated glucopyranosylium ion, which results from dissociation of the solvent-separated ion pair formed in the rate-limiting ionization reaction ($D_N^{\ddagger}$ + A_N). The implications that this model reaction have for the mode of action of retaining glycosyltransferases are discussed.

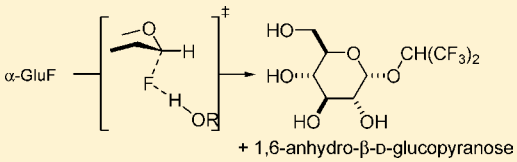

INTRODUCTION

Glycoconjugates are carbohydrate-containing structures that are involved in numerous biological processes, including many complex interactions such as the mediation and modulation of cell adhesion and cell signaling events.[1] As a consequence, research in this field has involved studying the main classes of enzymes responsible for either the addition or removal of sugar residues, namely, glycosyltransferases or glycosidases, respectively. The mechanisms by which the corresponding non-enzymatic reactions of glycosides occur can be used as a valuable cornerstone for the understanding of how enzymes accelerate these important biological reactions.[2,3] Central to a mechanistic discussion of these acetal substitutions is whether the reaction at the anomeric center occurs via an oxacarbenium ion intermediate.[4] In the context of the Winstein ion pair mechanism for solvolyses, the reaction of glucopyranosyl derivatives can occur through either a direct S_N2 reaction to give an inverted product or an S_N1 pathway in which product formation occurs at the stage of intimate, solvent-separated, or solvent-equilibrated ion pairs (Scheme 1).[5,6] Notably, the stereochemical outcome of these reactions can be influenced by the nature of the leaving group when oxacarbenium ion capture occurs on solvent-separated ion pairs. Recently, a substitution mechanism, which was originally labeled as an "intramolecular nucleophilic change (S_Ni)" by Ingold and co-workers,[7] in which the in vogue transition state structure that is drawn has partial bonding to both the nucleophile and the leaving group has received renewed attention. Such reactions have been well documented for substitutions at silicon; however, at carbon centers, the distinction between a classically defined S_Ni (D_N*D*A_N)[8] such as for the breakdown of chlorosulfites with retention of configuration and a concerted mechanism (A_ND_N) has become blurred in the literature.

The pioneering investigation by Sinnott and Jencks of the solvolysis products for the reactions of glucopyranosyl derivatives in mixtures of ethanol and trifluoroethanol (TFE) showed clearly that for substitution reactions on carbohydrates the product stereochemistry is influenced by the leaving group.[9] In particular, solvolysis of α-D-glucopyranosyl fluoride (α-GluF) gave trifluoroethyl products in which the retained diastereomer predominated, an observation from which Sinnott and Jencks concluded that generation of trifluoroethyl α-D-glucopyranoside could be regarded as a type of "internal return" involving the complex of the leaving group and solvent ($F^-\cdots HOCH_2CF_3$).[9]

With regard to carbohydrate-processing enzymes, the S_Ni mechanism is enjoying something of a renaissance. For example, it recently was concluded on the basis of a mechanistic study involving a transition state mimicry analysis, linear free energy relationships, and KIEs that for the retaining glycosyltransferase trehalose-6-phosphate synthase the catalyzed reaction involves a "front-face" mechanism.[10] In this study, the authors concluded that their results were consistent with the presence of either a metastable intermediate (S_Ni,

Received: October 4, 2011
Published: December 8, 2011

dx.doi.org/10.1021/ja209339j | J. Am. Chem.Soc. 2012, 134, 1212−1220

Scheme 1. General Mechanistic Scheme for the Reactions of α-D-Glycopyranosyl Derivatives[a]

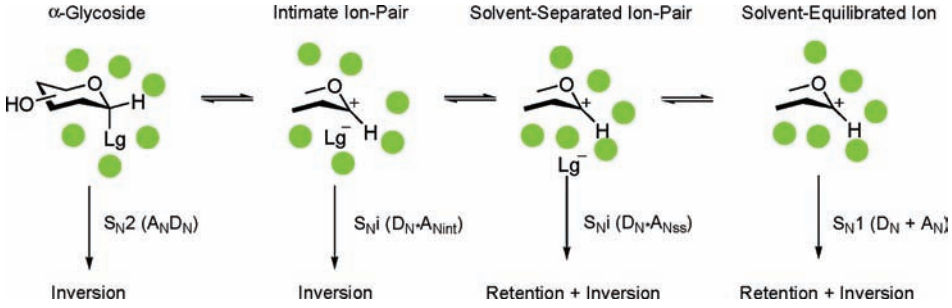

[a]The green circles represent solvent molecules.

$D_N{}^*A_{Nss}$) in a stepwise mechanism or a frontside concerted pathway with an exploded transition structure geometry (A_ND_N).[10] Other proposed mechanisms for retaining glycosyltransferases include standard double displacements in which the enzymatic nucleophile is either a carboxylate[11,12] or a side chain amide group.[13] The mechanism by which glycosyltransferases operate has recently been reviewed.[3,14]

To probe the intrinsic kinetic signatures for frontside substitution reactions on glucopyranosyl derivatives, we decided to examine the mechanism of solvolysis of α-GluF in the mildly acidic and non-nucleophilic solvent hexafluoro-2-propanol (HFIP). HFIP was selected because in comparison to TFE, used in the study by Sinnott and Jencks,[9] it is (i) more acidic, (ii) a stronger hydrogen bond donor, (iii) a more ionizing solvent, and (iv) less nucleophilic.[15] These solvent properties are expected to favor a greater selectivity for the formation of retained products. A panel of isotopically labeled α-D-glucopyranosyl fluorides (**1a–f**) was synthesized for the measurement of kinetic isotope effects on this solvolysis reaction. In addition, computational chemistry was employed to locate possible transition state structures using the experimental KIEs as restraints during modeling.

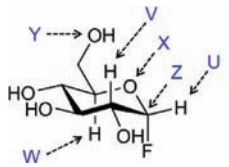

1a. U = ^{2}H
1b. V = ^{2}H
1c. W = ^{2}H
1d. X = ^{18}O
1e. Y = ^{18}O
1f. Z = ^{13}C

MATERIALS AND METHODS

Materials. 1,1,1,3,3,3-Hexafluoro-2-propanol (HFIP) and 1,1,1,3,3,3-hexafluoro-2-propan(ol-*d*) (HFIP-*d*), which were purified by using a standard procedure,[16] were purchased from Matrix Scientific and Aldrich, respectively. Water (^{18}O) was purchased from Olinax Inc. (98 atom % ^{18}O, batch 090215A4). 1,6-Anhydro-β-D-glucopyranose was purchased from TCI America. D-Glucose-1-^{13}C and D-glucose-2-^{2}H were purchased from Omicron Biochemicals, Inc. D-Glucose-1-^{2}H, D-glucose-5-^{2}H, and D-glucose-5-^{18}O were prepared according to known procedures.[17,18] α-D-Glucopyranosyl fluoride and its singly labeled isotopologues were prepared from the correspondingly labeled 1,2,3,4,6-penta-*O*-acetyl-α,β-D-glucopyranose in two steps using a known protocol.[19] All other reagents were purchased from Aldrich and used without purification. Thin-layer chromatography (TLC) was performed on aluminum-backed TLC plates precoated with Merck silica gel 60 F254. Compounds were visualized with UV light and/or staining with a *p*-anisaldehyde solution. Flash chromatography was performed using silica gel 60 (230–400 mesh). Solvents used in anhydrous reactions were dried and distilled immediately prior to use. THF was dried and distilled over sodium metal, and dichloromethane was dried and distilled over calcium hydride. For anhydrous reactions, all glassware was flame-dried and cooled under a nitrogen atmosphere immediately prior to use. NMR spectra were recorded on a Bruker 500 or 600 MHz spectrometer. Chemical shifts (δ) are listed in parts per million downfield from TMS. All NMR peak assignments are based on ^{1}H–^{1}H COSY and ^{1}H–^{13}C HMQC experiments; coupling constants are reported in hertz. Melting points were measured on a Gallenkamp melting point apparatus and are uncorrected. The synthesis of α-D-(6-^{18}O)glucopyranosyl fluoride (**1e**) requires 1,2,3,4,6-penta-*O*-acetyl-α,β-D-(6-^{18}O)glucopyranose (**3**), which was accessed in four steps beginning from 1,2-*O*-isopropylidene-α-D-glucofuranose in 43.2% yield overall as detailed below.

*1,2-O-Isopropylidene-6-^{18}O-α-D-glucofuranose (**2**).* A flame-dried flask was charged with 1,2-*O*-isopropylidene-α-D-glucofuranose (1.0 g, 4.54 mmol), ($^{18}O_2$)benzoic acid (544 mg, 4.38 mmol),[20] PPh_3 (2.38 g, 9.07 mmol), and anhydrous THF (75 mL). The resultant solution was cooled to 0 °C with an ice bath and treated with a solution of diethyl azodicarboxylate in toluene [40% (w/v), 5.0 mL, 10.46 mmol]. After the solution had been stirred at room temperature for 48 h, the volatiles were removed under reduced pressure and the crude residue was purified via flash chromatography [5:95 (v/v) MeOH/CH_2Cl_2] to afford the intermediate as a white solid. This material was treated with a solution of sodium methoxide in MeOH (~0.5 M, 25 mL) and was stirred until it was shown by TLC analysis [R_f = 0.28; 5:95 (v/v) MeOH/CH_2Cl_2] that reaction was complete. Following neutralization of the solution with Amberlite (H^+) resin, it was filtered and concentrated to afford the desired product as a white solid (520 mg, 54% yield over two steps): mp 160–161 °C (lit.[21] 161 °C); HRMS (M + Na^+) $C_9H_{16}O_5{}^{18}O_1$ requires *m*/*z* 245.0882, found *m*/*z* 245.0894.

*1,2,3,4,6-Penta-O-acetyl-α,β-D-(6-^{18}O)glucopyranose (**3**).* A solution of **2** (500 mg, 2.25 mmol) in water (15 mL) and acetone (15 mL) was treated with Amberlite (H^+) resin (1 g). The mixture was stirred while being heated to reflux for 3 h. After cooling, the resin was removed via filtration and rinsed with water (~20 mL). The filtrate was concentrated under reduced pressure, and the resultant syrupy residue was dissolved in pyridine (15 mL) and treated with acetic anhydride (5 mL). After being stirred at room temperature for 12 h, the solution was diluted with CH_2Cl_2 (50 mL) and washed sequentially with water (50 mL), cold 10% H_2SO_4 (50 mL), saturated $NaHCO_3$ (2 × 25 mL), and brine (25 mL). The organic layer was dried (Na_2SO_4) and concentrated to give a solid residue that was purified via column chromatography [1:1 (v/v) EtOAc/hexanes] to afford the title compound as a white foam (705 mg, 80% yield over two steps): HRMS (M + Na^+) $C_{16}H_{22}O_9{}^{18}O_1$ requires *m*/*z* 415.1097, found *m*/*z* 415.1109.

Product Isolation, Purification, and Identification. A 20 mL ampule was charged with **1** (220 mg, 1.21 mmol) and HFIP (10 mL). After being sealed, the reaction vessel was heated for 2 h in a steam bath. After the solution had cooled to room temperature, the volatiles were removed under reduced pressure and the crude residue was treated with pyridine (15 mL) and acetic anhydride (5 mL). After being stirred for 16 h at room temperature, the solution was diluted with CH_2Cl_2 (50 mL) and washed sequentially with cold 10% H_2SO_4

dx.doi.org/10.1021/ja209339j | J. Am. Chem.Soc. 2012, 134, 1212–1220

(50 mL), water (50 mL), saturated $NaHCO_3$ (50 mL), and brine (50 mL). The organic fraction was dried (Na_2SO_4) and concentrated to afford a syrupy residue. The protected HFIP solvolysis product (R_f = 0.29) and 2,3,4-tri-*O*-acetyl-1,6-anhydro-β-D-glucopyranose (R_f = 0.13) were purified via column chromatography [3:7 (v/v) EtOAc/hexanes]. Each product was treated with freshly prepared NaOMe in MeOH (~0.5 M, 10 mL). The reaction mixtures were neutralized with Amberlite IR-120+ resin (H^+ form), filtered, and concentrated to afford **4** (α-GluHFIP) and **5** (1,6-anhydro-β-D-glucopyranose).

*1,1,1,3,3,3-Hexafluoropropan-2-yl α-D-glucopyranoside (**4**):* mp 125−126 °C; $[\alpha]^{20}_D$ = +89.8 (*c* 0.017, H_2O); ^{1}H NMR (600 MHz, D_2O) δ 5.20 (d, *J* = 3.3, 1 H, H-1), 5.10 [m, 1 H, OC*H*(CHF_3)$_2$], 3.76 (m, 1 H, H-6), 3.74−3.64 (m, 3 H, H-3, H-6′, H-5), 3.57 (dd, *J* = 10.0, 3.8, 1 H, H-2), 3.40 (t, *J* = 9.5, 1 H, H-4); ^{13}C NMR (151 MHz, D_2O) δ 121.84 (q, J_{CF} = 62.6, $-CF_3$), 119.97 (q, J_{CF} = 65.5, $-CF_3$), 100.31 (C-1), 72.54, 72.00 (septet, J_{CF} = 32.4, $-CHCF_3$) 71.67, 70.34 (C-2), 68.55, 59.70 (C-6); HRMS (M + Na^+) $C_9H_{12}F_6O_6$ requires *m*/*z* 353.0430, found *m*/*z* 353.0443.

*1,6-Anhydro-β-D-glucopyranose (**5**):* $[\alpha]^{20}_D$ = −67.6 (*c* 0.017, H_2O) (lit.[22] = −66.0); ^{1}H NMR (600 MHz, D_2O) δ 5.38 (s, 1 H, H-1), 4.56 (d, *J* = 5.7, 1 H, H-5), 4.02 (d, *J* = 7.7, 1 H, H-6), 3.69 (m, 1 H, H-6′), 3.62−3.59 (m, 2 H, H-3, H-4), 3.45 (s, 1 H, H-2); ^{13}C NMR (151 MHz, D_2O) δ 100.96 (C-1), 75.78 (C-5), 72.01 (C-3), 70.32 (C-4), 69.69 (C-2), 64.71 (C-6); HRMS (M + Na^+) $C_6H_{10}O_5$ requires *m*/*z* 185.0420, found *m*/*z* 185.0420.

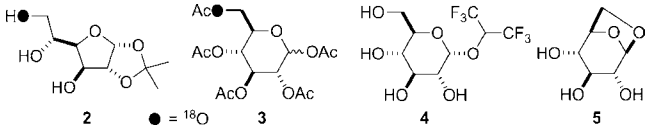

Solvolysis Product Stability. To show that α-GluHFIP is stable to the solvolysis conditions, α-GluHFIP (10 mg) was dissolved in HFIP (2 mL) and the solution sealed in an ampule that was heated in a steam bath for 12 h. Subsequent ^{1}H NMR spectroscopic analysis in D_2O of the nonvolatiles showed no 1,6-anhydroglucose. In addition, 1,6-anhydroglucose was shown to be stable under the reaction conditions by being heated a sealed ampule containing it (~1 mg), DMSO (15 μL), and 2,6-lutidine (4 μL) in HFIP (600 μL) at 100 °C for 2 h. After removal of the volatiles, the residue was dissolved in D_2O, and analysis by ^{1}H NMR spectroscopy showed that no reaction had occurred.

Activation Parameters. Ampules were charged with **1** (1 mg) in DMSO (5 μL), HFIP (1 mL), and 2,6-lutidine (1.5 μL). After being sealed, the ampules were heated in a "reflux chamber" equipped with a still pot containing an appropriate solvent. The temperature dependence of the reaction was determined by monitoring the rate of solvolysis at 56, 65, 82, and 100 °C by suspending the ampules in the vapors of boiling acetone, methanol, 2-propanol, and water, respectively. Samples were removed after various time intervals and cooled in an ice bath. The contents were transferred to a flask, from which the volatiles were removed under reduced pressure. The residue was dissolved in D_2O (650 μL) and analyzed by ^{1}H NMR spectroscopy. The anomeric proton chemical shifts for **1** (5.62 ppm), **4** (5.19 ppm), and **5** (5.38 ppm) were integrated and normalized. The normalized ratio of **1** was fit to a standard exponential one-phase decay using a nonlinear regression algorithm.

KIE Measurements. The α-^{2}H KIE was determined via ^{19}F NMR spectroscopy on a Bruker AVANCE III 500 MHz spectrometer.[20] A 5 mm NMR tube was charged with **1** (~1.5 mg), **1a** (~1.5 mg), DMSO-d_6 (15 μL), 1,4-difluorobenzene (1.5 μL), 2,6-lutidine (4.8 μL), and HFIP (650 μL). The NMR tube was flame-sealed, and an initial NMR spectrum was recorded with the sample temperature maintained at 298 K. Each quantitative proton-decoupled and -coupled ^{19}F NMR spectrum was acquired using a gated pulse sequence. Spectra consisting 128 scans (acquisition time of 0.35 s) were recorded with a recycle delay of 2.5 s between scans (6.1 min per spectrum). The baseline was corrected to remove baseline distortions that are typically associated with ^{19}F spectra using the Whittaker Smoother method found in MestReNova version 6.2. The ^{19}F signals corresponding to the internal standard 1,4-difluorobenzene (−124.27 ppm), **1** (−153.02 ppm), and **1a** (−153.74 ppm) were integrated. At various points throughout the course of the reaction, the same NMR tube was heated in a steam bath, cooled, and analyzed by ^{19}F NMR spectroscopy as described above. The resultant fraction of reaction (F_1) and individual peak areas were analyzed using a nonlinear least-squares fit to eq 1. Of note, the intense ^{19}F signal corresponding to HFIP (−78.66 ppm) does not overlap or interfere with the peaks of interest. All other KIEs were determined relative to the α-^{2}H KIE using eq 2

$$\frac{R}{R_0} = (1 - F_1)^{(1/\mathrm{KIE}-1)} \tag{1}$$

$$\mathrm{KIE} = \frac{^{1D}\mathrm{KIE}}{^{Rel}\mathrm{KIE}} = \frac{k_H}{k_x} \tag{2}$$

where ^{1D}KIE is the α-^{2}H isotope effect ($k_{unlabeled}/k_{1D}$) and ^{Rel}KIE (k_x/k_{1D}) is the relative isotope effect measured in the competitive experiment between **1a** and another labeled α-GluF. In these calculations, **1a** is treated as the "heavy" isotopologue such that the ratio of ^{1D}KIE and ^{Rel}KIE will give the KIE for x (i.e., x = **1b**). All calculations of standard deviations on KIE values computed using eq 2 involved standard propagation of the errors associated with the measured values of ^{1D}KIE and ^{Rel}KIE.[23]

Simultaneous Measurement of Three KIEs. A 5 mm NMR tube was charged with a solution of **1** (~0.3 mg), **1a** (~0.3 mg), **1b** (~0.3 mg), and **1f** (~0.6 mg) in DMSO-d_6 (50 μL), 1,4-difluorobenzene (0.2 μL), 2,6-lutidine (4.8 μL), and HFIP (600 μL). A protocol identical to that described above was used to measure 1-^{2}H, 2-^{2}H, and 1-^{13}C KIEs simultaneously.

Solvent KIE. A solution of **1** (16 mg) in DMSO-d_6 (75 μL) was added to a flask charged with HFIP (12 mL) and 2,6-lutidine (25 μL). The solution was distributed evenly into 14 prescored ampules that were subsequently sealed. Samples containing HFIP-*d* were prepared in an identical manner. These two sets of ampules were heated in a steam bath, and every 5 min, samples were removed and cooled in an ice bath. The observed rate constants were calculated as described in Activation Parameters.

THEORETICAL CALCULATIONS

Computational Analysis. Calculations for the HFIP solvolysis of α-GluF were performed using Gaussian 09 and the B3LYP method with a 6-31G* basis set.[24] All TS structures were calculated in the gas phase at 373 K. The α-GluF ground state structure was optimized beginning from several $^4C_1$ conformations to ensure that the calculated structure is a local minimum. In addition, ground state structures with a hydrogen bond between the C2 hydroxyl group and the anomeric fluorine atom were not considered to ensure that the intramolecular H−O···H hydrogen bonding arrangement, which mainly results from the system being calculated in vacuo, is the same in the TS as it is in the ground state. With regard to the TS structures for ionization of α-GluF, an HFIP molecule was positioned 4 Å from the fluoride leaving group and allowed to optimize. Subsequently, the C−F bond distance was incrementally increased and constrained to locate TS structures that had one imaginary frequency. In addition, a TS structure with an HFIP catalyzing the departure of the fluoride in a backside S_N2 reaction that generates 1,6-anhydro-β-D-glucopyranose was located by constraining the O6−C1 distance, a protocol that was necessary to prevent re-formation of the starting material. The ground state for 1,6-anhydroglucose was optimized from several starting geometries. Calculations were performed using the same conditions and level of theory. All TS structures were recalculated at the MP2(full)/6-31G* level of theory using the B3LYP geometric

dx.doi.org/10.1021/ja209339j | J. Am. Chem.Soc. 2012, 134, 1212−1220

constraints, although no further matching of experimental KIEs was performed in this study. KIEs for each putative TS structure were calculated using ISOEFF98.[25] Of note, scale factors of 0.9614 and 0.9427 were used for the B3LYP/6-31G* and MP2(full)/6-31G* calculations, respectively.[26]

The starting geometry used to probe computationally whether the epoxide (1,2-anhydro-α-D-glucopyranose) is a viable intermediate en route to the 1,6-anhydro product via a standard S_N2 reaction was generated by incorporating the following modifications into TS3: (i) the fluorine atom was removed, and (ii) the 2-OH group was transformed into an epoxide ring. All calculations were performed at the B3LYP/6-31G* level of theory without constraints. The bond distance between the epoxide oxygen and the hydrogen atom of a solvating HFIP molecule was incrementally varied by 0.05 Å from 1.79 to 1.04 Å. In addition, the O6−C1 distance was varied between 1.63 and 1.25 Å.

The equilibrium isotope effects (EIEs) for the formation of a solvent-equilibrated oxacarbenium ion could be computed from the vibrational frequencies of the cationic intermediate, the structure of which was calculated by optimizing the cation−HFIP complex in which the structure of TS1 without the fluoride ion was used as the starting point for minimization. The EIEs were then calculated using ISOEFF98.[25]

RESULTS AND DISCUSSION

Rate Constants and Product Studies. The rate constants for solvolysis of α-GluF in HFIP were measured at 56, 65, 82, and 100 °C and are summarized in Table S1 of the Supporting Information. The corresponding Eyring plot is shown in Figure 1, and the derived activation parameters are as follows: $\Delta H^{\ddagger}$ = 81.4 ± 1.7 kJ mol^{-1}, and $\Delta S^{\ddagger}$ = −90.3 ± 4.6 J mol^{-1} K^{-1}. The calculated activation parameters suggest that the solvolysis involves a highly ordered transition state, which likely results from solvation of the leaving group fluoride ion by the bulky HFIP solvent. Indeed, solvolysis of α-GluF in HFIP displays a negative entropy of activation greater than that of the corresponding reaction in water (−37 J mol^{-1} K^{-1}).[27]

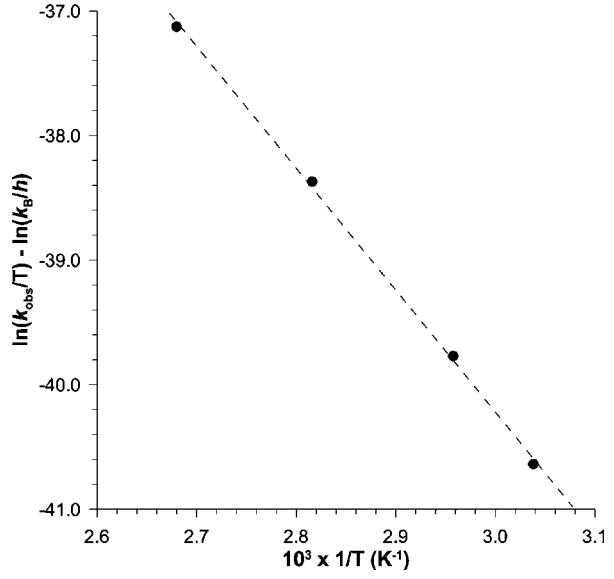

Figure 1. Eyring plot for the solvolysis of α-D-glucopyranosyl fluoride in 1,1,1,3,3,3-hexafluoro-2-propanol. The dashed line is the best linear fit to the rate constant data.

The identification of the two products of solvolysis of α-GluF (**1**) in HFIP at 100 °C were, after separation and purification, shown by ^{1}H NMR spectroscopy to be 1,1,1,3,3,3-hexafluoro-2-propyl α-D-glucopyranoside **4** (α-GluHFIP = 54.6 ± 2.2%) and 1,6-anhydro-β-D-glucopyranose **5** (45.4%) (Figures S1 and S2 of the Supporting Information show the ^{1}H and ^{13}C NMR spectra of α-GluHFIP, respectively). Of note, an identical product ratio, within experimental error, was noted in the NMR spectra for these solvolyses at all temperatures between 56 and 100 °C. For example, integration of the ^{1}H NMR spectrum for the solvolysis performed at 56 °C showed that α-GluHFIP constituted 55.8% of the binary mixture, while the remaining 44.2% was 1,6-anhydro-β-D-glucopyranose. Moreover, an identical product mixture was obtained when the solvolysis reaction was performed at 100 °C in HFIP-D (α-GluHFIP = 53.7 ± 1.2%; 1,6-anhydro-β-D-glucopyranose = 46.3%). The solvent deuterium KIE for the HFIP solvolysis of α-GluF at 100 °C was measured to be 1.68 ± 0.07 (see Materials and Methods for full details).

The formation of 1,6-anhydro-β-D-glucopyranose was shown not to involve a base-catalyzed S_N2 reaction involving 2,6-lutidine, which was added to neutralize the HF produced during solvolysis, as the rate of solvolysis was invariant as a function of base concentration (data not shown).

KIE Measurements. A slight modification to the "Direct NMR Method" developed by Chan et al. to measure ^{13}C and ^{18}O KIEs on the *Vibrio cholerae* sialidase-catalyzed hydrolysis of natural substrate analogues[20] was used in this study to evaluate the KIEs for the solvolysis of α-GluF in HFIP. Specifically, ^{19}F was the NMR active probe nucleus chosen to report on the changes in isotopologue ratios in the remaining starting material. That is, a pronounced ^{19}F chemical shift perturbation (~0.7 ppm) occurs upon substitution of the C1 proton with a deuteron (Figure 2). During the course of the solvolysis reaction, the ^{19}F signals corresponding to the internal standard (1,4-difluorobenzene) and the remaining starting isotopologues, for example, **1** and **1a**, were integrated. Figure 3 shows a stacked plot of the change in relative intensities of **1** and **1a** at various points throughout the course of the reaction. To ensure that the KIE values derived from the ^{19}F NMR spectroscopic experiments were accurate, the α-^{2}H KIE was measured seven times. Table S2 of the Supporting Information lists the individual KIE values measured for each experiment and the corresponding standard deviations.[23] In addition, it was verified that the KIE value was unaffected by nuclear

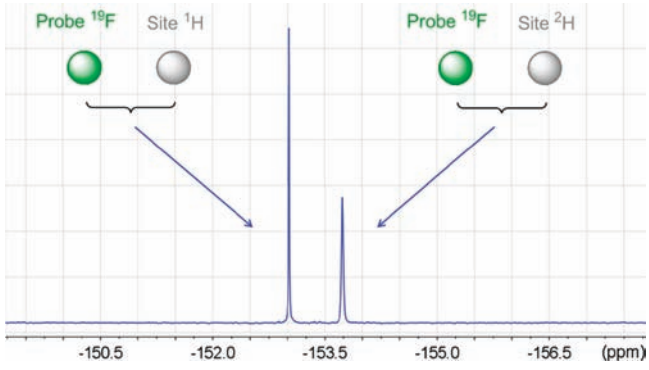

Figure 2. Proton-decoupled ^{19}F NMR spectrum of a mixture of α-D-glucopyranosyl fluoride (**1**) and α-D-(1-^{2}H)glucopyranosyl fluoride (**1a**) in 1,1,1,3,3,3-hexafluoro-2-propanol.

dx.doi.org/10.1021/ja209339j | J. Am. Chem.Soc. 2012, 134, 1212−1220

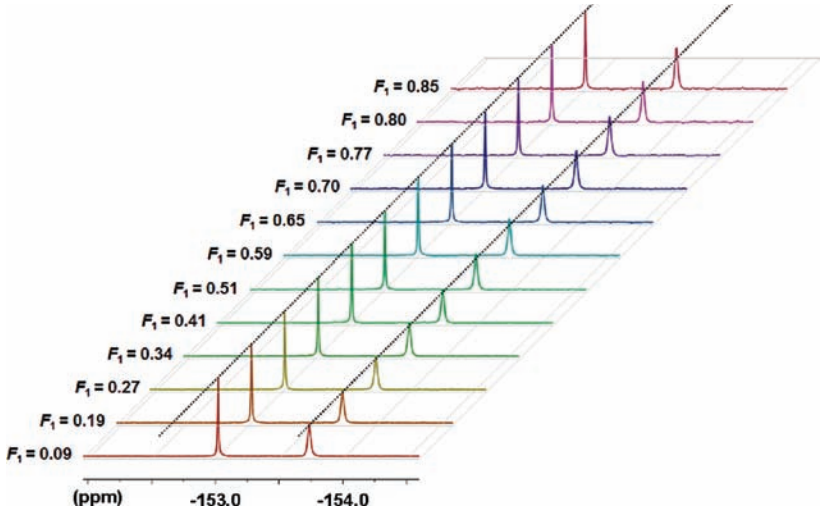

Figure 3. Stacked plot of proton-decoupled ^{19}F NMR spectra containing a mixture of **1** and **1a** in 1,1,1,3,3,3-hexafluoro-2-propanol as a function of the fraction of reaction of the unlabeled isotopologue (**1**). The two parallel dotted lines are for visualization of the change in relative peak intensity as the reaction progresses.

Overhauser effects (NOE) by performing the ^{19}F NMR spectroscopic experiment while accumulating data with an inverse-gated pulse sequence (Table S2, entry 7).

Although isotopic substitutions at positions farther from the fluorine atom do not necessarily produce a chemical shift perturbation sufficient to observe baseline resolution, it is possible to determine all other KIEs relative to the 1-^{2}H KIE. The relative ratio of each isotopologue (R) was determined by routine integration, and the fraction of reaction (F_1) was evaluated throughout the time course of the reaction using 1,4-difluorobenzene as an innocuous internal standard. These two parameters, R and F_1, are then fit to eq 1 to determine the ^{Rel}KIE (k_x/k_{1D}). The KIE of interest can then be calculated using eq 2 (Table S3 of the Supporting Information). Panels a and b of Figure 4 show the least-squares fits to eq 1 for typical

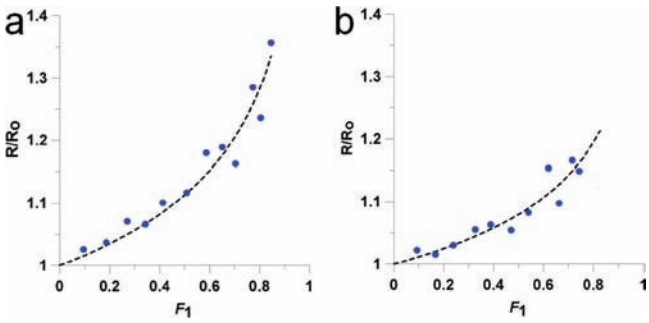

Figure 4. Plots of the change in integrated peak intensity ratio (R/R_0) vs F_1 for the competitive KIE measurements: (a) data from an experimental measurement of k_H/k_{1D} and (b) data from an experimental measurement of k_{2D}/k_{1D}.

data sets for the competition reactions between **1** and **1a** and between **1b** and **1a**, respectively.

To verify that the calculated KIE values were indeed accurate, we performed a single NMR experiment in which the 1-^{2}H, 2-^{2}H, and 1-^{13}C KIEs were measured simultaneously. That is, the NMR solution contained three isotopologues in addition to unlabeled α-GluF (Figure 5). Of note, as it was necessary to reduce the initial concentrations of each α-GluF isotopologue by approximately 6-fold to limit signal overlap, sequential

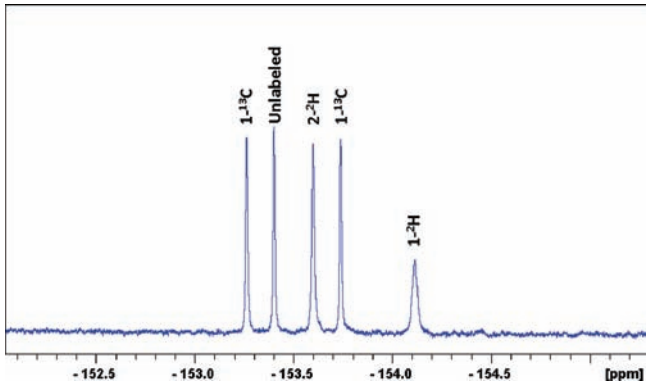

Figure 5. Proton-decoupled ^{19}F NMR spectrum of a solution of **1** (~0.3 mg), **1a** (~0.3 mg), **1b** (~0.3 mg), and **1f** (~0.6 mg) in HFIP. All peaks in the spectrum are labeled with the appropriate assignment.

spectra were combined using the "fidadd" function in TopSpin 2.1 when the signal-to-noise ratio deteriorated to an unsatisfactory level, a protocol that reduced the total number of experimental data points used in the fit to eq 1. The determined KIE values for this experiment are also listed in Table 1, while the fits to the experimental data are shown in Figures S3–S5 of the Supporting Information.

Table 1. Mean Individual Measurements of KIEs on the Solvolysis of α-D-Glucopyranosyl Fluoride in HFIP at 100 °C and the Corresponding Standard Deviations[a]

compd	site of substitution	KIE and SD	simultaneous KIE
1a	1-^{2}Hα deuterium	1.185 ± 0.006	1.190 ± 0.006
1b	2-^{2}Hβ deuterium	1.080 ± 0.010	1.076 ± 0.007
1c	5-^{2}Hγ deuterium	0.987 ± 0.007	
1d	5-^{18}O ring oxygen	0.997 ± 0.006	
1e	6-^{18}O nucleophile oxygen	1.003 ± 0.007	
1f	1-^{13}C anomeric	1.008 ± 0.007	1.000 ± 0.002

[a]Also given are the results from a single simultaneous measurement of three KIEs.

^{13}C KIE. The anomeric ^{13}C KIE for the solvolysis of α-GluF in HFIP is 1.008 ± 0.007 (Table 1; the value from a single

dx.doi.org/10.1021/ja209339j | J. Am. Chem.Soc. 2012, 134, 1212–1220

multiple-KIE experiment is 1.000 ± 0.002), which is in the typical range associated with a dissociative S_N1-like reaction.[18,28,29] If the 1,6-anhydroglucose that results from these solvolyses is formed by a concurrent S_N2 pathway, a reaction that should exhibit KIEs between 1.03 and 1.08,[27−29] it would be expected that the ^{13}C KIE would be significantly larger than that measured. As such, these results are inconsistent with the notion that two independent pathways are involved. Moreover, the anomeric ^{13}C KIE for the solvolysis of α-GluF is of the same magnitude as those reported for the acid-catalyzed hydrolyses of methyl α-D-glucopyranoside (1.007 ± 0.001)[18] and methyl α-D-xylopyranoside (1.006 ± 0.001).[30] It is therefore likely that these reactions have similar TS structures and that the solvolysis of α-GluF in HFIP has a late TS with significant C−F bond cleavage.

^{18}O KIEs. The experimental 5-^{18}O and 6-^{18}O KIEs are 0.997 ± 0.006 and 1.003 ± 0.007, respectively. Of note, the small inverse endocyclic ^{18}O KIE is of a magnitude similar to that reported for the hydrolysis of methyl α-D-glucopyranoside,[18] and these values are significantly different from those of the conformationally more flexible methyl xylopyranosides[30] or those from sialidase-catalyzed hydrolysis reactions,[20] where more extensive charge delocalization onto the ring oxygen atom is the likely cause of the reported ^{18}O KIEs of 0.978−0.986. In other words, these small inverse KIE measurements for the solvolysis of α-GluF indicate that the TS geometry possesses a poor $n_p \rightarrow \pi$ orbital overlap.[18]

With respect to the measured value for the C6 oxygen atom, few examples of ^{18}O KIEs have been reported in the literature where the isotopic substitution is in the nucleophile;[31,32] it is clear that on the basis of the measured value of 1.003 ± 0.007 for the 6-^{18}O isotopologue and those calculated for the various possible transition states (vide infra) it is impossible to differentiate between TSs solely on the basis of the magnitude of this effect.

Secondary Deuterium KIEs. The measured α-secondary deuterium KIE (α-SDKIE) for the solvolysis of α-GluF in HFIP is 1.185 ± 0.006 (Table 1; the value from a single multiple-KIE experiment is 1.190 ± 0.006), whereas the corresponding α-SDKIE for its spontaneous hydrolysis is 1.142 ± 0.007,[27] a reaction that occurs via an exploded S_N2 (A_ND_N) TS.[27,33] These KIEs are primarily associated with weakening of an out-of-plane bending vibration as the steric crowding at the reaction becomes weaker on approach to a carbenium ion-like transition state, although it important to remember that maximal α-SDKIE values depend on the identity of the leaving group.[34−36]

The β-secondary deuterium KIEs (β-SDKIE), which originate from hyperconjugative weakening of the C−H/(D) bond with the developing empty p orbital at the anomeric center, for HFIP solvolysis and hydrolysis of α-GluF are 1.080 ± 0.010 (Table 1; the value from a single multiple-KIE experiment is 1.076 ± 0.007) and 1.067 ± 0.008,[27] respectively. The magnitude of β-SDKIEs has been used to provide insights into TS conformations,[18,27] as hyperconjugation is an angle-dependent phenomenon that varies as a function of $\cos^2(\theta)$, where θ is the dihedral angle between the C−H/(D) bond and the developing p orbital on the anomeric center.

Finally, the measured γ-secondary deuterium KIE (γ-SDKIE) is 0.987 ± 0.007, an effect that traditionally has been considered to originate from inductive effects; however, it is now clear that inductive isotope effects are exceedingly small.[37,38]

Solvent Kinetic Isotope Effect. Normal solvent deuterium KIEs ($k_{SOH}/k_{SOD} > 1$) are associated with general catalyzed reactions, while inverse values ($k_{SOH}/k_{SOD} < 1$) indicate the occurrence of specific catalysis. The observed KIE (k_{SOH}/k_{SOD} = 1.68 ± 0.07) is consistent with proton transfer occurring as part of the rate-limiting transition state for solvolysis, and this certainly involves protonation of the departing fluoride ion.[39]

General Mechanistic Scheme. The important observations that the product ratio is independent of the solvent (HFIP or HFIP-*d*) yet the rate of solvolysis is dependent require either that the rate-determining and product-determining steps in a sequential S_N1-like mechanism are not the same or that if the products are formed in two parallel reactions they have the same SKIE. All data are consistent with a unified mechanism that involves formation of a solvent-separated oxacarbenium ion intermediate that partitions to either α-GluHFIP by collapse of the ion pair [$D_N^{\ddagger}$*A_{Nss} (Scheme 1)] or 1,6-anhydro-β-D-glucopyranose by dissociation to give a solvent-equilibrated ion pair in which the oxacarbenium ion has a significant lifetime before intramolecular capture by the C6 hydroxyl group ($D_N^{\ddagger}$ + A_N). The critical observation that partitioning to the product is independent of both temperature and solvent (HFIP or HFIP-*d*) requires that the processes that determine the partition ratio have similar activation enthalpies and solvent deuterium isotope effects. In the current example, we suggest that this involves solvent reorganization at the stage of the solvent-separated ion pair to give either the retained product by intramolecular capture (k_c) or 1,6-anhydroglucose via a dissociation (k_{-d}) into a solvent-equilibrated oxacarbenium ion that ultimately undergoes intramolecular capture (Scheme 2).

Scheme 2. Possible Mechanisms for the Solvolysis Reactions of α-D-Glucopyranosyl Fluoride in Hexafluoro-2-propanol

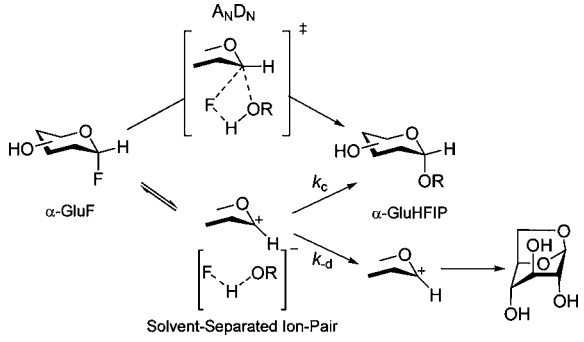

Indeed, carbenium ion lifetimes in HFIP have been reported to be extended by factors of approximately 10^4 and 10^8 in comparison to those in TFE and water, respectively.[40] For instance, the rate constants for solvent capture (k_s) of the diphenylmethyl carbenium ion, at 20 °C, are 1.3 × 10^9, 3.2 × 10^6, and ∼1 × 10^1 s^{-1} in water,[41] TFE,[42] and HFIP,[43] respectively. Given that the estimated lifetime of the glucopyranosylium ion in aqueous solutions is ∼1−3 ps,[44,45] the expected lifetime of this cation in HFIP is certainly in the range that would allow for the formation of solvent-equilibrated ions.

Of note, no evidence was obtained to indicate that any inverted solvolysis product (β-GluHFIP) was formed during these reactions. On the basis of the analysis described above that the key partitioning steps between the two reaction products occur at the stage of the solvent-separated ion pair, the two possibilities that exist for the formation of the 1,6-anhydro-β-D-glucopyranose are (i) direct intramolecular

dx.doi.org/10.1021/ja209339j | J. Am. Chem.Soc. 2012, 134, 1212−1220

capture of the solvent-equilibrated glucopyranosylium ion by the 6-hydroxyl group and (ii) neighboring group capture to give the 1,2-epoxide that in a subsequent step forms the anhydro product. At present, we are experimentally unable to distinguish between these two possibilities; however, we tried computationally to investigate whether an S_N2-type reaction was feasible between the 1,2-anhydro (epoxide) and the 1,6-anhydro product. Of note, all calculations, including starting geometries expected to favor formation of the 1,6-anhydro product, gave instead an optimized structure of the 1,2-epoxide that was hydrogen bonded to an HFIP molecule. At present, we suggest, on the basis of these calculations, that the 1,6-anhydro-β-D-glucopyranose results from an intramolecular capture of the glucopyranosylium ion rather than by an intramolecular A_ND_N reaction of 1,2-anhydro-α-D-glucopyranose.

Computational Analysis. Two TS structures for the solvolysis reaction, TS1 and TS2, were located computationally with the suite of experimental KIEs being used as restraints. First, TS1 involves an HFIP-catalyzed cleavage of the carbon–fluorine glycosidic bond, and this transition state precedes the formation of an oxacarbenium ion intermediate (Figure 6).

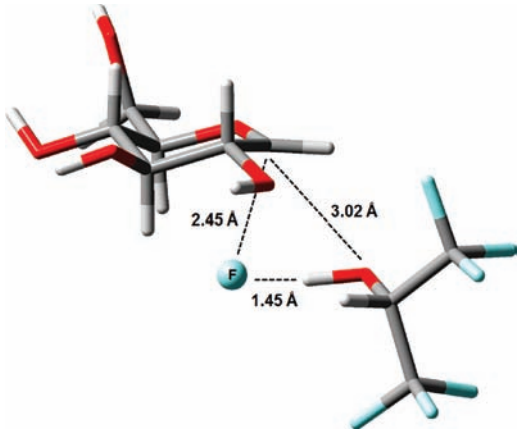

Figure 6. Transition state structure TS1 for the $D_N^{\ddagger}*A_{Nss}$ reaction of α-D-glucopyranosyl fluoride in 1,1,1,3,3,3-hexafluoro-2-propanol. The transition state structure was determined in vacuo by hybrid density functional theory implemented in Gaussian 09 using the B3LYP functional and the 6-31G* basis sets. The distances among the leaving group fluoride, the anomeric carbon, and the catalytic solvent molecule are shown.

Second, TS2 entails a coupled fluoride ion departure and a nucleophilic attack of the catalyzing HFIP (Figure 7). The computed KIE values for both transition states are summarized in Table 2 along with the experimentally determined values.

A single transition state (TS3) was located for formation of the second reaction product 1,6-anhydroglucopyranose, via a concerted frontside S_N2 reaction (Figure 8 and Table 2). For this model, it was necessary to fix the O6–C1 bond distance to prevent starting material, α-GluF, from being generated. TS3 incorporates an HFIP solvent molecule into the model and thus allows proton transfer to occur during fluoride ion departure. Listed in Tables S4–S11 of the Supporting Information are the Cartesian coordinates of the computed ground state and TS structures and the associated energies and imaginary frequencies. Of note, a transition state model that did not contain an HFIP acting as a general acid catalyst for the intramolecular backside A_ND_N reaction was also located, and details of this TS (TS4) are given in the Supporting

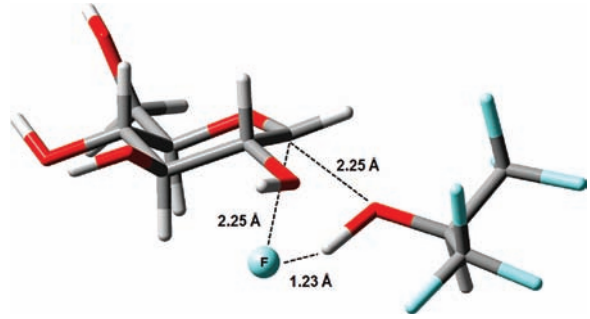

Figure 7. Transition state structure TS2 for the frontside A_ND_N reaction of α-D-glucopyranosyl fluoride in 1,1,1,3,3,3-hexafluoro-2-propanol. The transition state structure was determined in vacuo by hybrid density functional theory implemented in Gaussian 09 using the B3LYP functional and the 6-31G* basis sets. The distances among the leaving group fluoride, the anomeric carbon, and the catalytic solvent molecule are shown.

Information (Figure S6 and Tables S12–S15). Listed in Tables S16 and S17 of the Supporting Information are selected bond distances and angles of the calculated TSs.

In addition, the structure of a glucopyranosylium ion–HFIP complex was computed (Table S18 and Figure S7 of the Supporting Information), and the EIEs calculated for the formation of this oxacarbenium ion–molecule complex are listed in Table 2.

Transition State Analysis. Using the experimental KIEs as constraints, the two possibilities for the S_Ni ($D_N^{\ddagger}*A_{Nss}$ and A_ND_N) mechanism were modeled by varying the C–F bond distance (r_{C-F}) in 0.05 Å increments between 2.30 and 2.60 Å and between 2.20 and 2.40 Å for TS1 and TS2, respectively. Both structures adopt a flattened chair conformation with the main difference between the two TS models being the position and orientation of HFIP. Of these two models, the predicted KIEs for TS1 ($D_N^{\ddagger}*A_{Nss}$) more closely match the experimental values (Table 2). Critical features of TS1 include (i) extensive C–F bond fission (r_{C-F} = 2.45 Å) and (ii) the moderate transfer of protons from the solvating HFIP to the fluoride ion. When r_{C-F} is increased beyond 2.60 Å, the computed structure is minimized to an oxacarbenium ion–hexafluoroisopropoxide ion pair and HF. With regard to TS2, an archetype of a coupled "frontside" S_Ni mechanism, the computed TS involves a noticeably different geometry at the anomeric center, with the sum of the three bond angles at C1 being 351.8° and 353.4° for the B3LYP and MP2 calculations, respectively, whereas, for TS1, in which the anomeric center is almost planar, the corresponding sums are 358.5° and 359.0° for the B3LYP and MP2 calculations, respectively. For the TS2 model when the C–F bond distance is increased past 2.25 Å, an extrusion of HF occurs with simultaneous formation of α-GluHFIP.

Of note, the experimental anomeric ^{13}C KIE (k_{12}/k_{13} = 1.008) is not modeled particularly well by either of the two models (TS1 or TS2). Indeed, no TS that possessed a single imaginary frequency that gave a better calculated agreement with this KIE was located. However, a calculated structure [TS5 (Figure S8 of the Supporting Information)] that possesses two imaginary frequencies, which following minimization became TS1, has a calculated anomeric ^{13}C KIE that is identical to the experimental value. The two imaginary frequencies associated with TS5 involve (i) C2–OH bond rotation (−287.9 cm^{-1}) and (ii) C–F bond cleavage (−180.1 cm^{-1}). The two transition state models for the $D_N^{\ddagger}*A_{Nss}$ reaction (TS1 and TS5) are

dx.doi.org/10.1021/ja209339j | J. Am. Chem.Soc. 2012, 134, 1212–1220

Table 2. Experimental KIEs for α-D-Glucopyranosyl Fluoride HFIP Solvolysis and the Corresponding Computational Values

position	exptl KIE	TS1 B3LYP[a]	TS1MP2[b]	TS2 B3LYP[a]	TS2MP2[b]	TS3 B3LYP[a]	TS3MP2[b,c]	TS5 B3LYP[a]	oxacarbenium−HFIP complex[a,d]
1-^{2}H	1.185	1.1806	1.1709	1.1007	1.1131	1.0568	1.0513	1.1553	1.1342
2-^{2}H	1.080	1.1111	1.0982	1.0913	1.0872	1.0278	1.0241	1.1029	1.0747
5-^{2}H	0.987	0.9859	0.9932	0.9750	0.9740	0.9980	1.0037	0.9802	0.9979
5-^{18}O	0.997	0.9971	0.9933	0.9941	0.9912	0.9949	0.9961	0.9952	0.9928
6-^{18}O	1.003	1.0000	1.0001	0.9996	0.9996	1.0058	1.0065	0.9993	0.9980
1-^{13}C	1.008	1.0192	1.0188	1.0200	1.0189	1.0373	1.0383	1.0081	1.0054

[a]Calculated at the B3LYP/6-31G* level of theory. [b]Calculated at the MP2(full)/6-31G* level of theory. [c]Single-point calculation using the geometry from the B3LYP/6-31G* calculation. [d]Calculated equilibrium isotope effects (EIEs).

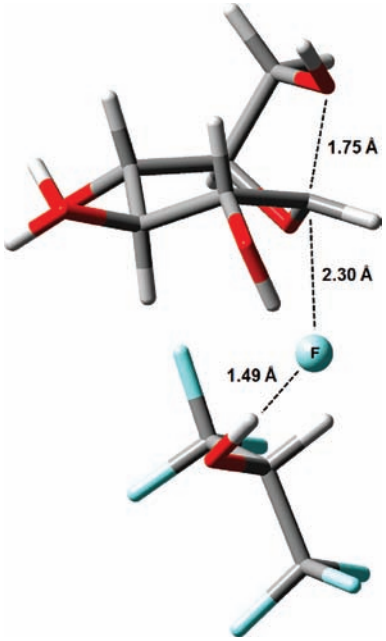

Figure 8. Transition state structure TS3 for a hypothetical backside A_ND_N reaction of α-D-glucopyranosyl fluoride in 1,1,1,3,3,3-hexafluoro-2-propanol to give 1,6-anhydro-β-D-glucopyranose as the product. The transition state structure was determined in vacuo by hybrid density functional theory implemented in Gaussian 09 using the B3LYP functional and the 6-31G* basis sets. The distances among the leaving group fluoride, the anomeric carbon, the catalytic solvent molecule, and the C6 hydroxyl group are shown.

remarkably similar (Table S15 of the Supporting Information) in spite of the differences in the calculated anomeric ^{13}C KIEs.

Biological Implications. The results of this study clearly show that in a non-nucleophilic environment the glucopyranosylium ion has a sufficiently long lifetime to permit conformational interconversions of the pyranosyl ring. The reported anomeric ^{14}C KIE (k_{12}/k_{14} = 1.023),[10] when converted[28] to the expected value for the ^{13}C isotopologue (k_{12}/k_{13} = 1.012), and the α-secondary deuterium KIE for the retaining glucosyltransferase (trehalose-6-phosphate synthase)[10] are remarkably similar to the values reported here for the solvolysis of α-GluF. In contrast, the transferase reaction exhibits a β-secondary deuterium KIE, albeit with a non-natural nucleophile,[10] that is significantly larger than both the experimental value for solvolysis of α-GluF and the computed values for TS1 (and TS5; $D_N^{\ddagger}{*}A_{Nss}$) and TS2 (frontside A_ND_N). Unfortunately, we are unable to measure a leaving group isotope effect for solvolysis of α-D-glucopyranosyl fluoride for a comparison with the reported $^{18}V/K$ value.[10] In this recent paper, Lee et al. noted that the glucosyl transfer reaction displayed a moderate sensitivity to the pK_a of the conjugate acid of the acceptor nucleophile (Brønsted, β_{nuc} = 0.54).[10] Taking all these observations together, we suggest that the reported results for the biological glucose transfer reaction, when taken in the context of our experimental and computed KIE values, are consistent with the biological process occurring in a stepwise fashion with the kinetically significant step being capture of the glucopyranosylium ion intermediate that is formed in the presence of the bound nucleophilic acceptor, i.e., a $D_N{*}A_N^{\ddagger}$ mechanism.[46] That is, the observed KIEs for isotopic substitution on the UDP-glucose ring are composites of the equilibrium isotope effect for formation of the glucopyranosylium ion (calculated EIEs for the formation of a glucopyranosylium ion are listed in Table 2) and the kinetic trapping of this ion by the sugar acceptor, which must occur via an early TS. A comment on our analysis of why the model reaction has rate-limiting dissociation while nucleophilic attack is a kinetically significant step in the biological reaction is justified. Specifically, leaving group departure in the case of α-D-glucopyranosyl fluoride has been shown by Banait and Jencks to involve enforced general catalysis because the glucopyranosylium cation does not have a significant lifetime in the presence of a nonsolvated fluoride ion,[39] which in our example requires the acidic solvent to promote fluoride departure. However, once at the stage of the solvent-separated ion pair, the back reaction to re-form α-D-glucopyranosyl fluoride becomes negligible because once the small F^- anion is solvated it is only weakly nucleophilic; i.e., formation of the solvent-separated ion pair is rate-limiting. With regard to retaining glycosyltransferases, we suggest that leaving group departure (UDP in the case of trehalose-6-phosphate synthase) does not require significant general acid catalysis from the weakly acidic bound sugar acceptor hydroxyl group because the pyrophosphate component is tightly coordinated by positively charged residues,[47] which by themselves likely provide sufficient catalysis for leaving group departure. We note that Ardèvol and Rovira, on the basis of a QM/MM calculation for trehalose-6-phosphate synthase, recently concluded that the mechanism involves the formation of a short-lived cationic intermediate and that the highest point on the reaction free energy profile involves nucleophilic attack on the anomeric center by the acceptor hydroxyl group, a process that is catalyzed by the UDP leaving group,[48] and that Goedl and Nidetzky transformed the active site of sucrose phosphorylase into a glycosyltransferase mimic by mutation of the enzymatic active site.[49]

■ CONCLUSIONS

The solvolysis reaction of α-D-glucopyranosyl fluoride in hexafluoro-2-propanol occurs via rate-limiting C−F bond cleavage that is coupled to proton transfer for a solvent

dx.doi.org/10.1021/ja209339j | J. Am. Chem.Soc. 2012, 134, 1212−1220

molecule. The formed solvent-separated ion pair forms the product via two separate reaction channels: (i) collapse of the ion pair gives retained solvolysis product ($D_N^{\ddagger}$*A_{Nss}), and (ii) dissociation of the ion pair gives a solvent-equilibrated glucopyranosylium ion that subsequently reacts to give the inverted product 1,6-anhydro-β-D-glucopyranose ($D_N^{\ddagger}$ + A_N).

■ ASSOCIATED CONTENT

Supporting Information

Complete citation for ref 24, Tables S1−S16, ^{1}H (Figure S1) and ^{13}C (Figure S2) NMR spectra of 1,1,1,3,3,3-hexafluoro-2-propyl α-D-glucopyranoside, and Figures S3−S6. This material is available free of charge via the Internet at http://pubs.acs.org.

■ AUTHOR INFORMATION

Corresponding Author

E-mail: bennet@sfu.ca

■ ACKNOWLEDGMENTS

We thank the Mizutani Foundation for Glycoscience for a grant to support this research.

■ REFERENCES

(1) Taylor, M. E.; Drickamer, K. *Introduction to Glycobiology*; Oxford University Press: Oxford, U.K., 2003.
(2) Sinnott, M. *Comprehensive biological catalysis: A mechanistic reference*; Academic Press: San Diego, 1998.
(3) Sinnott, M. *Carbohydrate chemistry and biochemistry: Structure and mechanism*; RSC Publishing: Cambridge, U.K., 2007.
(4) Bennet, A. J.; Kitos, T. E. *J. Chem. Soc., Perkin Trans. 2* **2002**, 1207−1222.
(5) Winstein, S.; Appel, B.; Baker, R.; Diaz, A. *Spec. Publ.—R. Soc. Chem.* **1965**, *19*, 109−130.
(6) Lowry, T. H.; Richardson, K. S. *Mechanism and theory in organic chemistry*, 3rd ed.; Harper & Row: New York, 1987.
(7) Cowdrey, W. A.; Hughes, E. D.; Ingold, C. K.; Masterman, S.; Scott, A. D. *J. Chem. Soc.* **1937**, 1252−1271.
(8) Guthrie, R.; Jencks, W. P. *Acc. Chem. Res.* **1989**, *22*, 343−349.
(9) Sinnott, M. L.; Jencks, W. P. *J. Am. Chem. Soc.* **1980**, *102*, 2026−2032.
(10) Lee, S. S.; Hong, S. Y.; Errey, J. C.; Izumi, A.; Davies, G. J.; Davis, B. G. *Nat. Chem. Biol.* **2011**, *7*, 631−638.
(11) Monegal, A.; Planas, A. *J. Am. Chem. Soc.* **2006**, *128*, 16030−16031.
(12) Soya, N.; Fang, Y.; Palcic, M. M.; Klassen, J. S. *Glycobiology* **2011**, *21*, 547−552.
(13) Fritz, T. A.; Hurley, J. H.; Trinh, L. B.; Shiloach, J.; Tabak, L. A. *Proc. Natl. Acad. Sci. U.S.A.* **2004**, *101*, 15307−15312.
(14) Lairson, L. L.; Henrissat, B.; Davies, G. J.; Withers, S. G. *Annu. Rev. Biochem.* **2008**, *77*, 521−555.
(15) Schadt, F. L.; Schleyer, P. V.; Bentley, T. W. *Tetrahedron Lett.* **1974**, 2335−2338.
(16) Perrin, D. D.; Armarego, W. L. F. *Purification of laboratory chemicals*, 3rd ed.; Pergamon Press: Oxford, U.K., 1988.
(17) Hardick, D. J.; Hutchinson, D. W. *Bioorg. Med. Chem. Lett.* **1994**, *4*, 409−414.
(18) Bennet, A. J.; Sinnott, M. L. *J. Am. Chem. Soc.* **1986**, *108*, 7287−7294.
(19) Hayashi, M.; Hashimoto, S.; Noyori, R. *Chem. Lett.* **1984**, 1747−1750.
(20) Chan, J.; Lewis, A. R.; Gilbert, M.; Karwaski, M. F.; Bennet, A. J. *Nat. Chem. Biol.* **2010**, *6*, 405−407.
(21) Gramera, R. E.; Park, A.; Whistler, R. L. *J. Org. Chem.* **1963**, *28*, 3230−3231.
(22) Montgomery, E. M.; Richtmyer, N. K.; Hudson, C. S. *J. Org. Chem.* **1945**, *10*, 194−198.
(23) Taylor, J. R. *An introduction to error analysis: The study of uncertainties in physical measurements*; University Science Books: Mill Valley, CA, 1982.
(24) Frisch, M. J. et al. *Gaussian 09*, revision A.02; Gaussian, Inc.: Wallingford, CT, 2009.
(25) Anisimov, V.; Paneth, P. *J. Math. Chem.* **1999**, *26*, 75−86.
(26) Scott, A. P.; Radom, L. *J. Phys. Chem.* **1996**, *100*, 16502−16513.
(27) Zhang, Y.; Bommuswamy, J.; Sinnott, M. L. *J. Am. Chem. Soc.* **1994**, *116*, 7557−7563.
(28) Melander, L. C. S.; Saunders, W. H. J. *Reaction rates of isotopic molecules*; Wiley: New York, 1980.
(29) Lee, J. K.; Bain, A. D.; Berti, P. J. *J. Am. Chem. Soc.* **2004**, *126*, 3769−3776.
(30) Indurugalla, D.; Bennet, A. J. *J. Am. Chem. Soc.* **2001**, *123*, 10889−10898.
(31) Cassano, A. G.; Anderson, V. E.; Harris, M. E. *Biochemistry* **2004**, *43*, 10547−10559.
(32) Marlier, J. F. *J. Am. Chem. Soc.* **1993**, *115*, 5953−5956.
(33) Banait, N. S.; Jencks, W. P. *J. Am. Chem. Soc.* **1991**, *113*, 7951−7958.
(34) Shiner, V. J. Jr.; Rapp, M. W.; Halevi, E. A.; Wolfsberg, M. *J. Am. Chem. Soc.* **1968**, *90*, 7171−7172.
(35) Harris, J. M.; Hall, R. E.; Schleyer, P. v. R. *J. Am. Chem. Soc.* **1971**, *93*, 2551−2553.
(36) Shiner, V. J. Jr.; Dowd, W. *J. Am. Chem. Soc.* **1971**, *93*, 1029−1030.
(37) Perrin, C. L.; Ohta, B. K.; Kuperman, J. *J. Am. Chem. Soc.* **2003**, *125*, 15008−15009.
(38) Perrin, C. L.; Ohta, B. K.; Kuperman, J.; Liberman, J.; Erdelyi, M. *J. Am. Chem. Soc.* **2005**, *127*, 9641−9647.
(39) Banait, N. S.; Jencks, W. P. *J. Am. Chem. Soc.* **1991**, *113*, 7958−7963.
(40) O'Ferrall, R. M. *Adv. Phys. Org. Chem.* **2010**, *44*, 19−122.
(41) Chateauneuf, J. E. *J. Chem. Soc., Chem. Commun.* **1991**, 1437−1438.
(42) McClelland, R. A.; Kanagasabapathy, V. M.; Steenken, S. *J. Am. Chem. Soc.* **1988**, *110*, 6913−6914.
(43) McClelland, R. A.; Cozens, F. L.; Li, J. H.; Steenken, S. *J. Chem. Soc., Perkin Trans. 2* **1996**, 1531−1543.
(44) Amyes, T. L.; Jencks, W. P. *J. Am. Chem. Soc.* **1989**, *111*, 7888−7900.
(45) Huang, X.; Surry, C.; Hiebert, T.; Bennet, A. J. *J. Am. Chem. Soc.* **1995**, *117*, 10614−10621.
(46) Zhang, Y.; Luo, M. K.; Schramm, V. L. *J. Am. Chem. Soc.* **2009**, *131*, 4685−4694.
(47) Errey, J. C.; Lee, S. S.; Gibson, R. P.; Fleites, C. M.; Barry, C. S.; Jung, P. M. J.; O'Sullivan, A. C.; Davis, B. G.; Davies, G. J. *Angew. Chem., Int. Ed.* **2010**, *49*, 1234−1237.
(48) Ardèvol, A.; Rovira, C. *Angew. Chem., Int. Ed.* **2011**, *49*, 10897−10901.
(49) Goedl, C.; Nidetzky, B. *ChemBioChem* **2009**, *10*, 2333−2337.